

Hydrological impact of widespread afforestation in Great Britain using a large ensemble of modelled scenarios

Marcus Buechel ¹, Louise Slater ¹ & Simon Dadson^{1,2}

Ambitious afforestation proposals in the last decade target potential flood mitigation and carbon storage benefits but without a systematic, large-scale (>1000 km²) quantitative evaluation of their impacts on streamflow. Here, we assess the impact of afforestation on streamflow across twelve diverse catchments (c.500-10,000 km²) using a high-resolution land-surface model with a large ensemble of afforestation scenarios. Afforestation consistently decreases median and low streamflow. Median modelled flow is reduced by 2.8% ± 1.0 (1 s.d.), or 10 mm yr⁻¹ ± 2.1 (1 s.d.), for a ten-percentage point increase in catchment broadleaf woodland. We find no nationally-consistent reduction of extreme floods. In larger catchments, planting extent is a stronger control on streamflow than location. Our results suggest that despite its potential environmental and societal benefits, widespread afforestation may inadvertently reduce water availability, particularly in drier areas, whilst only providing a modest reduction in extreme flood flows.

¹School of Geography and the Environment, University of Oxford, South Parks Road, Oxford OX1 3QY, UK. ²UK Centre for Ecology & Hydrology, Crowmarsh Gifford, Wallingford OX10 8BB, UK. ✉email: marcus.buechel@ouce.ox.ac.uk

Much debate exists about the possible large-scale land-cover change impacts on catchment hydrology across temporal and spatial scales^{1,2}. Afforestation is suggested to have many co-benefits such as improving biodiversity, air and water quality, providing timber, enhancing human well-being and reducing flood risk^{3,4}. Widespread afforestation is often suggested as a solution for achieving Net Zero (balancing carbon emissions with removal) by numerous groups including the UK government^{5,6}. However, there is a limited understanding of how effective woodland is for Natural Flood Management in modifying water fluxes and stores over large catchments^{1,7}. Impacts of land cover on hydrology are particularly important to understand due to changing streamflow regimes both in the UK and globally^{8–11}.

Land cover exerts strong localised controls on the water balance and streamflow timings within a catchment that can be difficult to detect over larger scales^{2,12}. Numerous studies have investigated the influence of afforestation on hydrology, including plot-scale studies to understand infiltration rates and groundwater levels, and small catchment studies evaluating the impact of land-cover change on streamflow and water quality^{13–15}. However, these studies are often smaller than 1000 km² in size, and it is unknown whether the impacts of afforestation may scale up over larger catchments, given its complex influence on streamflow^{16–18}. Furthermore, few systematic evaluations exist of how afforestation location and extent may influence catchment hydrology across a wide range of climatic and physiographic conditions^{19,20}.

This study is a theoretical assessment of the extent to which afforestation extent and location in catchments predominantly over 1000 km² in size may increase or decrease streamflow across temperate catchments in the British Isles. We hypothesise that: (i) increasing afforestation extent should proportionally reduce streamflow at all exceedances^{16,21}; (ii) catchments may be more hydrologically responsive to certain afforestation locations such as upland compared to lowland regions^{1,2}; (iii) catchment properties such as climate and soil types may differentiate a catchment's hydrological response to afforestation²². Our work is the first, to our knowledge, to employ a high-resolution 1 km² physics-based land-surface model to quantify the impact of afforestation on streamflow across multiple catchments using a large ensemble of land-cover scenarios. This approach allows us to isolate drivers influencing catchment sensitivity, determine individual hydrological processes altered by widespread afforestation, elucidate the uncertainty generated by afforestation location and most importantly find the impact of afforestation over large spatial extents on streamflow. Beyond the British Isles, our results describe the influence of afforestation on temperate catchment hydrology.

We focus on twelve diverse catchments (areas covering 511–9931 km²) which capture multiple hydrological regimes, drainage patterns, soil, and land-cover types to understand catchment properties influencing streamflow response to afforestation (Fig. 1 and Supplementary Table S1). Using the Joint UK Land Environment Simulator (JULES) run at a 30 minute timestep, we simulate the hydrological implications of a large ensemble of broadleaf afforestation scenarios^{23,24} (“Methods”). JULES simulates carbon, water and energy fluxes at the land surface when driven with a time series of meteorological data. Further details about the model setup can be found in the “Methods”.

Systematic criteria were used to generate up to 288 broadleaf afforestation scenarios per catchment for planting within grasslands (“Methods”), in line with afforestation scenarios that show improved pastures and rough grasslands will be the most likely initial afforestation locations in the UK²⁵. However, we note this approach does not consider other factors such as the socio-economic implications of afforestation location. Initially, we identify separate planting locations in each catchment using either stream order^{26,27} (relative size of stream in a catchment) or

propensity for saturation²⁸ (how likely a location is to be wet after rainfall) (“Methods”). Stream order varies from one to seven (small to large stream) and propensity for saturation from one to five (low-to-high saturation level). We create watersheds (catchment boundaries) that are both within, and outside, each of the defined catchment planting locations (Supplementary Fig. S1). Broadleaf woodland planting was then either random, with ~25 and 50% randomly distributed within the chosen locations, or around existing land cover at 25 and 50 m buffers. Discussion exists over where to plant woodland in relation to existing land cover. To investigate these planting locations, we systematically add woodland around watercourses^{29,30}, urban areas^{31,32} and existing broadleaf woodland^{4,33}. Afforestation according to these planting criteria generated between 234 and 288 scenarios and between 0 and c. 40 percentage point increase in broadleaf woodland per catchment (Supplementary Fig. S2). However, owing to the available space and catchment area the same extent of maximum afforestation could not be achieved in all catchments; nor do we account for the possible effect of forest stand age on catchment hydrology¹³. A large ensemble of scenarios provides evidence to ascertain whether a hydrological change in catchments is primarily driven by planting location or extent, and to quantify the variability, or uncertainty, induced by afforestation across catchments.

To characterise afforestation influence on streamflow we use eight hydrologic metrics^{34,35}. For analysing extreme and average streamflow, we calculate the top 1% (very high flow), 5% (high flow), 50% (median flow), 90% (low flow) and 95% (very low flow) quantiles of daily flows for the period 2000–2010. This period allows us to observe the impact of land-cover change in a flood-rich period^{36,37} and avoid uncertainty in catchment hydrology when comparing scenarios to original land cover that would substantially change over longer periods. We compute the slope of the flow duration curve, to quantify flow variability^{38,39}; median streamflow elasticity, to measure catchment streamflow response to yearly changes in precipitation^{40,41}; and runoff ratio to calculate water balance changes related to streamflow and evaporation⁴². To determine catchment hydrological responsiveness to afforestation, we calculate the median regression slope of changes in streamflow metrics for every percentage point increase in afforestation over the study period, for each catchment and watershed afforestation area⁴³. This regression slope is a proxy for catchment responsiveness to afforestation and is used to infer the median change in a hydrologic metric due to afforestation in a catchment. For each catchment, Spearman's rank correlation is calculated between the quantified catchment sensitivity to afforestation and catchment attributes⁴⁴. To establish the impact and significance of different planting locations on hydrologic metrics according to catchment and land-cover location we undertake a one-way analysis of variance (ANOVA) test.

Results and discussion

Afforestation extent influence on streamflow. Afforestation on average reduces streamflow linearly at all streamflow quantiles within JULES (Fig. 1). At the highest flows, we find a small reduction of streamflow with increases in broadleaf woodland (median reduction of $1.3\% \pm 0.6$ (one standard deviation) and $1.4\% \pm 0.6$ for the top 1% and 5% flows respectively, per ten-percentage point increase in woodland) (refer to Supplementary Table S2 for percentage and absolute values). These percentage changes in the high flows are relatively small compared to flood peak magnitudes, meaning a substantial area of the catchment would need to be afforested before an appreciable reduction in flow is observed. The correlation strength is moderate ($\rho = -0.46 \pm 0.17$ across individual catchments (Supplementary Table S3)) suggesting

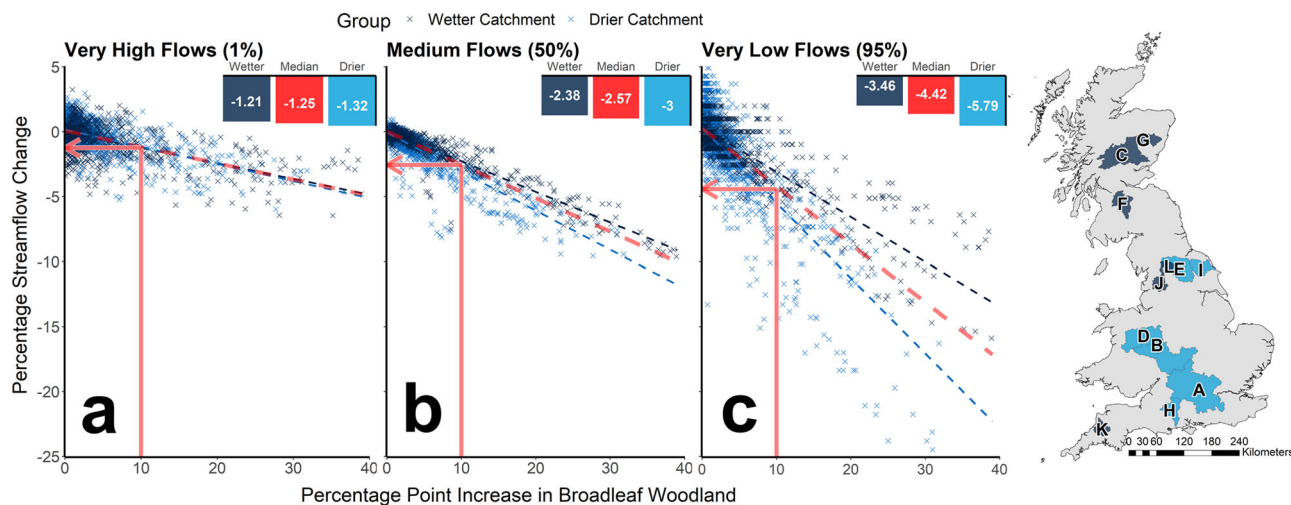


Fig. 1 Effect of afforestation on high, median and low flows across Great Britain. Three scatter graphs illustrating the percentage reduction in flow quantile levels for each percentage point of woodland planted in the different catchments. Reduction in (a) the top 1% of flows, (b) the median flows and (c) the 95% quantile of daily flows. Each data point represents an afforestation scenario in a single catchment. Dashed red lines represent the median reductions in the different flow quantiles for all catchments. Dark blue represents the six wetter catchments (mean precipitation 3.11–4.16 mm day⁻¹) and lighter blue, the six drier catchments (1.99–2.55 mm day⁻¹). Bars show the reduction in each flow level per ten-percentage point increase in broadleaf woodland for the different groups as well as the median reduction for all catchments in red. Catchment locations are shown on the right and the lettering code can be found in Supplementary Table S1.

afforestation location and other factors can affect streamflow reduction at the highest flows (Fig. 1a–c). There appears to be a weaker correlation between afforestation extent and high-flow reductions in small catchments compared to the largest (e.g., Tamar, $\rho = -0.35$; Severn-HB, $\rho = -0.77$ (Supplementary Table S3)). This finding suggests the impact of afforestation location is important in smaller catchments but in the larger catchments, the locational impact is diluted, making it more difficult to disentangle afforestation location^{45,46}. Targeted afforestation for flood management may therefore be detectable in smaller catchments, but become less impactful as the broadleaf woodland extent is scaled up over larger catchments^{1,7}. Greater uncertainty exists in how afforestation extent and location will impact streamflow in smaller catchments, with a wide range of possible responses. However, there is a more predictable hydrological response to the land-cover change in the largest catchments, regardless of the location change.

Afforestation impact on catchment hydrology varies seasonally, with large decreases in runoff in the winter, spring, and autumn months and no decrease or minor increases in summer months within JULES (Supplementary Fig. S3). An increase in high flows for some catchments coincides with the timing of the highest flows during the summer months. Our simulations suggest that this increase in high flows is due to an increase in topsoil moisture leading to greater levels of saturation-excess overland flow following periods of high-intensity rainfall. In all periods, there is increased evaporation from intercepted water stored in the canopy, but this increase in topsoil moisture is primarily driven by a decrease in soil evaporation (Supplementary Fig. S4). Particularly in the winter and spring periods, an increase in soil evaporation results from the loss of leaves from the broadleaf woodland, followed by regrowth. In the model, reduced canopy cover increases the exposure of the soil surface to incoming short-wave radiation and reduces aerodynamic resistance, leading to an increase in potential evaporation. With broadleaf planting on grasslands, there is increased soil infiltration, soil and canopy evaporation and transpiration rates, and so we therefore find a commensurate reduction in both the surface and subsurface runoff. In contrast, in the summer months a decrease in modelled

soil evaporation increases topsoil moisture (because the increase in canopy foliage reduces soil exposure to short-wave radiation and surface wind speed). As broadleaf woodland can achieve a higher leaf area index than the grasslands, the increase in topsoil moisture enhances saturation levels at rainfall interception (at the soil) and thus surface runoff. It should also be noted the increase in topsoil moisture may be due to differences in the root structures of broadleaf woodland and grasslands represented in JULES. While broadleaf woodland is modelled to have a root depth of 3 m, grasslands have root depths of 0.5 m, resulting in a potential overdrying of the topsoil.

Afforestation extent reduces simulated median and low flows the most, with $-2.8\% \pm 1.0$ and $-4.3\% \pm 3.1$ respectively per ten-percentage points of afforestation (Supplementary Table S2). Strong correlations between median and low-flow reduction and afforestation suggest extent has a stronger influence on reducing streamflow than location, and this finding is supported by previous studies ($\rho = -0.83 \pm 0.12$, $\rho = -0.75 \pm 0.15$ (Supplementary Table S3))^{12,39,47–49}. Each percentage point of afforestation in a catchment reduces the median flow by $1.0 \text{ mm yr}^{-1} \pm 0.21$. Reduction of the median and low flows is primarily due to modelled increases in evaporation (Supplementary Fig. S4), which is either from the woodland canopy or the soil surface when deciduous trees shed their leaves. Small increases in the woodland area increase the lowest flows on average the most for the smallest catchments, due to the increased summer topsoil moisture, which is not balanced by the increased evaporation in subsequent months. As the woodland area increases, there is a greater reduction in overall flows and more water leaves the catchment model domain by evaporation, reducing the lowest flow quantiles. Downstream of small afforestation locations there would not be any major disturbances to streamflow, and it may provide slight buffering against drought conditions.

Catchment response to afforestation extent is also clear using the flow-regime metrics (runoff ratio, slope of the flow duration curve and catchment elasticity). We find a reduced contribution of rainfall in streamflow with a decrease in the runoff ratio ($-1.9\% \pm 0.6$ per ten-percentage points of afforestation) as reported in previous studies^{14,50}. Modelled flow regimes become

more variable with strong decreases in low and lesser decreases in high-flow quantiles, increasing the slope of the flow duration curve ($1.1\% \pm 0.7$ per ten-percentage points of afforestation). The greater variance between flow-regime variability and afforestation suggests planting location more strongly controls streamflow regimes than extent ($\rho = -0.46 \pm 0.23$ (Supplementary Table S3)). Catchment discharge response to yearly changes in rainfall also decreases with broadleaf afforestation by modulating rainfall input to a catchment (median reduction in catchment elasticity of $-3.5\% \pm 1.2$ per ten-percentage points of afforestation). Changes in a catchment's rainfall regime would therefore be less detectable in streamflow observations. These findings highlight the fact that simulations of future streamflow using physics-based models depend not only on climatic changes but also land-cover changes. Without the inclusion of land-cover changes, considerable uncertainty will be introduced into projections of future flooding, drought and water management⁵¹.

Afforestation location influence on streamflow. ANOVA reveals highly significant differences ($P < 0.01$) in simulated flow reductions for all flow quantile levels when planting across the different stream orders, apart from the very highest flows ($F(1,670) = 5.3$, $P = 0.022$) (Fig. 2a). This highly significant difference in streamflow reduction across stream orders for the hydrologic metrics is due to differences in the largest and smaller streams, suggesting woodland acreage matters more than planting location. To emphasise, when the same area of broadleaf is planted for each stream order there is no highly significant difference between orders ($P > 0.01$). Runoff reduction according to stream order is also highly significant as seen in the runoff ratio and catchment elasticity ($F(1,670) = 17.93$, $P < 0.01$; $F(1,670) = 14.01$, $P < 0.01$). Again, these differences are due to planting between the largest and the smaller streams. Flow-regime variability differences by stream order location were not as significantly different ($F(1,670) = 5.11$, $P = 0.0241$) suggesting catchment planting area does not consistently lead to differences in flow-regime variability.

Planting according to different saturation areas led to significantly distinct reductions in streamflow for both the median and low flows in JULES when planting extent is not constant ($F(1,478) = 4.89$, $P < 0.01$; $F(1,478) = 11.11$, $P < 0.01$) (Fig. 2b). However, the difference between saturation areas is less significant for all other flow quantiles and when planting extent becomes fixed in each area, the differences between streamflow reductions are not significant ($P > 0.01$). This means selecting afforestation sites within areas that are more or less likely to become saturated may not necessarily lead to different hydrological responses downstream, if planting the same acreage. However, afforestation effects differ the most between the least and most likely areas of saturation when planting acreage is not fixed ($P = 0.011$), with greater reductions in the modelled runoff ratio in the least saturated areas. Benefits observed at small afforestation-plot scales may not size up to larger catchments and could have a negligible impact on reducing the highest flows.

Planting location, around urban, broadleaf, watercourses, or randomly, leads to different simulated streamflow dynamics (Fig. 2c) even when the area planted is constant. Not planting according to existing land cover greatly reduces streamflow at all flow quantiles compared with planting around the three existing land-cover types. The difference in planting area location is greatest for low-flow quantiles (ANOVA $P < 0.001$) compared with high-flow quantiles ($P < 0.01$). Overall, no single best planting location could be identified around existing land covers if trying to provide Natural Flood Management benefits⁵². We find consistent, minimal differences in streamflow when planting around urban

and watercourses, across all flow quantiles. Planting location also significantly reduces catchment runoff ($P < 0.001$) for both runoff ratio and catchment elasticity; the largest differences occur when planting is not according to existing land cover but when it was random. However, location effect on flow-regime variability is more nuanced, with notable differences between planting around urban, watercourse locations and randomly.

The difference in streamflow reduction is not significantly different when planting woodland inside and outside of the various drainage basin locations (Supplementary Fig. S5). Often it is debated whether interventions to reduce maximum flows are more effective in the headwaters or the valley floor downstream¹. This modelling study finds no compelling difference in streamflow, including extreme flood flow changes, when similar acreage is planted in the headwaters or the valley floor. However, in our study only one tree type is planted, so location may matter more for other tree types. In addition, our model does not simulate the effects of forest management techniques such as ditching and coppicing that might also have an influence on streamflow^{49,53}.

Catchment properties altering streamflow sensitivity to afforestation. Catchment climate exerts a strong influence on the hydrological response to afforestation in different types of catchments when comparing model results to their attributes. There are strong associations between climate properties and median flow reduction (Table 1). As a catchment's average rainfall (and runoff ratio) increase, afforestation has a smaller effect on streamflow reduction in JULES (Fig. 1a–c). We find planting broadleaves have less of an impact on low-flow conditions and droughts in wetter locations, and greater response in drier areas. Drier catchments are more likely to show decreases in runoff from afforestation, due to increased rates of potential evapotranspiration and water usage, as seen in other studies^{21,49,50} (Fig. 1). A negative association with catchment aridity emphasises this point. In situations of high rainfall and thus high runoff events, the same runoff generation processes will be present in a catchment with and without afforestation. In these situations, land cover will only have a minimal impact on flow reduction. Here, the strong correlation with catchment elevation is likely influenced by differences in average rainfall ($\rho = 0.8$, $P = 0.0032$). Few of the catchment properties shown in Table 1 exhibit significant correlations with catchment response to afforestation at the high and low flows. This could be due to differences in planting location with catchment attributes not capturing the temporal and spatial elements of runoff generation mechanisms influenced by afforestation or the greater variability in extremes. The catchment area has a strong negative association between high-flow reduction and afforestation potentially due to the greater relative reduction in the specific discharge of larger compared to smaller catchments.

There are not many significant associations between simulated catchment hydrology changes and catchment soil attributes (Table 1). This suggests that catchment soil properties may have a minimal role in altering catchment hydrology response to afforestation, at least in the JULES model. However, the slight significant negative association between soil depth to bedrock and changes in streamflow regimes with afforestation suggests afforestation may alter longer-term hydrological fluxes. In catchments with deeper soils, where subsurface flow dominates, afforestation is likely to reduce the subsurface component of streamflow, decreasing runoff ratio and catchment elasticity whilst increasing flow-regime variability. A similar effect can also be seen in the low flows, albeit slight. This effect may be overemphasised in JULES owing to its uniform

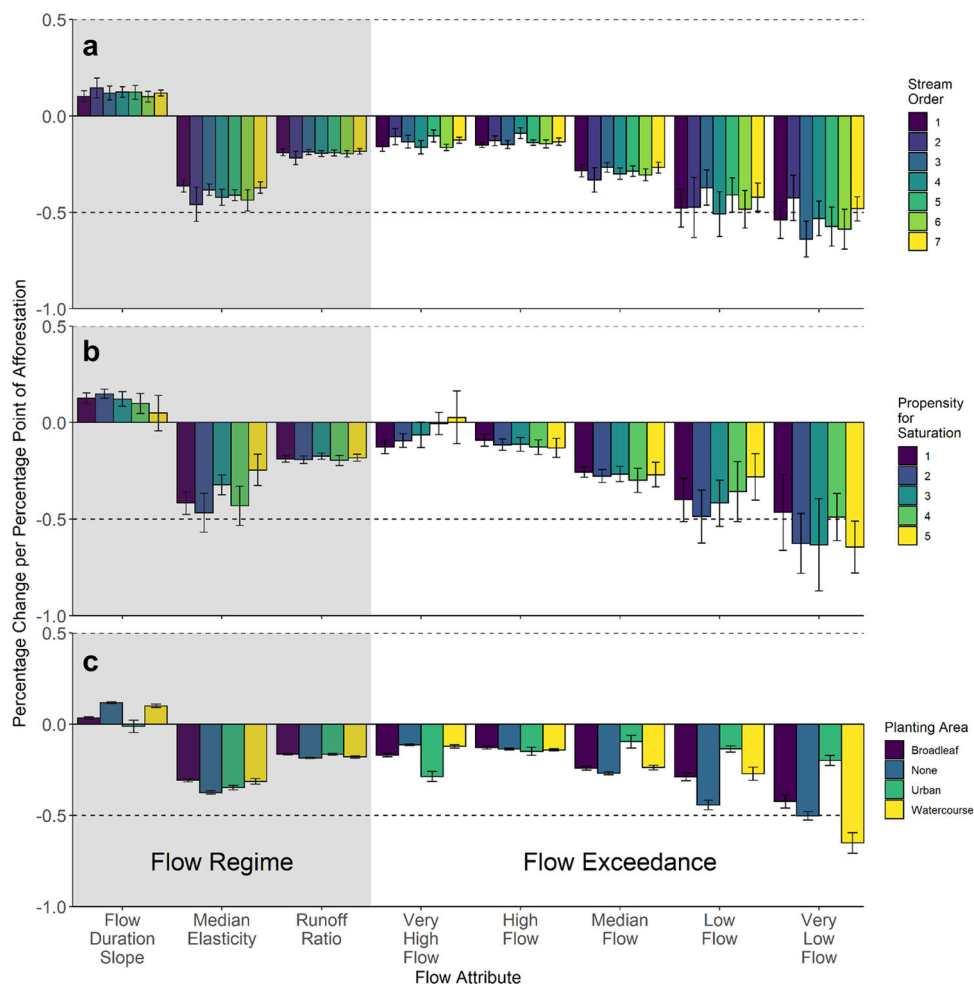


Fig. 2 Percentage streamflow change for each percentage point of afforestation. Sensitivity of catchment hydrology to afforestation in relation to (a) stream order, (b) propensity for saturation, (c) planting area. “None” in planting area indicates the absence of preferential planting location, i.e. planting randomly at 25 and 50% within a catchment area. Left three metrics (grey shading) reflect flow regimes, whereas those on the right represent five flow quantiles. The vertical axis indicates the median quantile regression slope for the percentage change in the hydrologic indicator per percentage point increase in broadleaf woodland. For example, a quantile coefficient of -1 would represent a median 1% decrease for each percentage point increase in woodland. Each bar represents the mean quantile coefficient for all catchments and the error bars represent the standard error.

soil depth and so could be due to runoff generation mechanisms using topographic slope.

Conclusions

This study has quantified potential afforestation impacts on temperate catchment hydrology in Great Britain using a high-resolution land-surface model. We find afforestation reduces streamflow at all flow quantiles with a clearer impact observed at median and low flows than high flows in twelve catchments over 500 km². When attributing changes in streamflow, afforestation location in the catchment can influence the highest and lowest streamflow extremes, particularly in smaller catchments. We find the extent of afforestation is more important than its location, particularly for the median flows. Simulated catchments with low rainfall and deep soils are more hydrologically responsive to afforestation than others in our chosen catchments. We show the effects of widespread afforestation on streamflow over multiple spatial scales within catchments can be significant and thus are important to include when establishing projections of hydrological change. These results provide quantitative insight into key water management decisions regarding the extent and location of afforestation in temperate regions and suggest caution is required when advocating widespread tree planting to mitigate future

hydro-climatic change or to attempt to control flooding in large catchments.

Methods

Catchment locations and input data. To determine the impact of afforestation on catchment hydrology we select twelve varied catchments from across the British Isles (Supplementary Material-S1 and Fig. 1). These catchments capture a range of hydrological regimes, drainage patterns and catchment soil and land-cover properties to determine how such factors may influence catchment response to afforestation. Being predominantly >1000 km² in area (ranging from 511 to 9931 km² in size), they are adequately represented in a hydrological model to integrate processes at a 1 km² spatial resolution^{54,55}. Two catchments are nested within larger ones, the Ure within the Ouse, and the Severn at Bewdley (Severn-B) within the Severn at Haw Bridge (Severn-HB) (Fig. 1).

The period 2000–2010, a flood-rich period for the British Isles^{36,37}, is chosen to assess afforestation influence on streamflow as it allows us to avoid the uncertainty that would be associated with land-cover changes over a longer period when comparing to baseline results. This length of the simulation period also reduces the computational demand with a large ensemble of land-cover scenarios. Accordingly, the CEH land-cover map for the year 2000⁵⁶, in the form of the CHES-land dataset⁵⁷, is used to provide configurational datasets specifying soil hydraulic and thermal properties, vegetation characteristics, and orography, for the model at a 1 km² spatial resolution for the unaltered land-cover scenarios. This dataset has successfully been used in other studies^{55,58}. The 25 m rasterised land-cover map is reclassified into eight different land-cover types (Supplementary Tables S4 and S5) and used to derive afforestation scenarios related to land cover before being converted to a percentage land-cover fraction at a 1 km² spatial resolution.

Table 1 Sensitivity to afforestation with catchment properties.

	Mean precipitation (mm day ⁻¹)	Found in the literature as Aridity Index	Found in the literature as Baseflow Index	Soil porosity	Soil hydrological conductivity (cm day ⁻¹)	Soil depth to bedrock (m)	Area (km ²)	Mean elevation (m.a.s.l.)
Flow duration slope	-0.25	0.34	-0.33	0.09	-0.08	0.67*	-0.12	-0.27
Median elasticity	0.71*	-0.77**	-0.57	-0.14	0.41	-0.71*	-0.38	0.73*
Runoff ratio	0.9***	-0.8***	-0.55	-0.01	0.33	-0.76*	-0.47	0.7*
Very low flow	0.56	-0.5	-0.19	0.1	0.04	-0.62*	-0.13	0.31
Low flow	0.31	-0.42	-0.24	-0.59*	0.15	0.13	0.52	0.61*
Median flow	0.77*	-0.82**	-0.44	-0.41	0.41	-0.54	-0.08	0.81**
High flow	0.43	-0.42	-0.43	0.33	0.25	-0.46	-0.85**	0.24
Very high flow	0.38	-0.39	-0.28	-0.22	0.6*	-0.24	-0.48	0.4

Spearman correlation between catchment attributes and percentage change in hydrologic metric with afforestation extent. Asterisks indicate significance: *P < 0.05; **P < 0.005; ***P < 0.0005. The aridity index is characterised as the ratio between catchment mean precipitation and mean potential evapotranspiration. A larger correlation table can be found in Supplementary Fig. S6.

To provide the required meteorological driving data, we use the CHES-met dataset⁵⁹ which includes long-wave and short-wave radiation, air temperature, specific humidity and pressure. The 50 m CEH Integrated Hydrological Digital Terrain Model elevation data is used to derive topographical and catchment attributes as well as catchment boundaries and river networks⁶⁰. Soil hydraulic information comes from the Harmonised World Soil Database and was made uniform across each grid cell⁶¹.

The model. The Joint UK Land Environment Simulator (JULES) is a physically based land-surface model that simulates the fluxes of carbon, water and energy at the land surface when driven by a time series of the atmospheric data^{23,24}. Multiple studies have used JULES before including the investigation into evapotranspiration drivers across Great Britain^{58,62}, atmospheric river formation over Europe⁶³, the impact of solar dimming and carbon dioxide on runoff⁶⁴ and developing river routing algorithms with a Regional Climate Model⁶⁵. JULES is routinely used at the Met Office, where it is coupled with several other models to understand future changes globally and across the UK, by bridging the atmosphere, land surface and ocean⁶⁶. This study is predominantly a theoretical, scenario-based modelling study designed to draw out general principles and to quantify the relation between afforestation and hydrological response, and as such the results are not intended to provide detailed guidance for specific practical actions.

The use of a process-based model enables us to investigate physical explanations for the hydrological impacts of changes in land cover and the explicit representation of vegetation that will influence fluxes, partitioning and storages within the realm of epistemic uncertainty for other conceptual and hydrological models where vegetation is not included. JULES models both plant phenology and canopy storages^{23,24}. When changing the plant functional type in JULES, both the properties of the above-ground vegetation (such as canopy height and leaf area index) and the soil infiltration factor and the root depth are altered²³. However, there are several caveats that must be considered with this approach. First, the model configuration used in the present study is uncoupled from the atmosphere and so large-scale land-cover changes cannot alter nearby weather⁶⁷. Second, each grid cell is hydrologically separated from adjacent cells, with streamflow and runoff hydrologically uncoupled from the rest of the system. Soil water also does not flow between grid cells. Third, soil thermal and hydraulic properties are uniform across a grid cell. This reduces the impact of hydrological pathways within a cell and the interaction of vegetation with these varying soil types that could have ramifications at multiple temporal and spatial scales. For example, within the cell there may be vegetation that is water-stressed (e.g. valley sides) compared with vegetation where water is not limited (e.g. floodplain) which would change how much transpiration is possible and thus runoff⁶⁸.

Precipitation in the model is partitioned by vegetation and when it reaches the soil surface it is portioned into either infiltration excess overland flow, at a rate controlled by the hydraulic conductivity of the soil, or saturation-excess overland flow as determined by the Probability Distributed Model (PDM)^{69,70}. Throughfall (T_F) through the canopy is dependent on the rainfall and the existing water in the canopy:

$$T_F = P \left(1 - \frac{C}{C_m} \right) \exp \left(- \frac{\epsilon_r C_m}{P \Delta t} \right) + P \frac{C}{C_m} \tag{1}$$

where P is the rainfall rate ($\text{kg m}^{-2} \text{s}^{-1}$), C is the amount of water in the canopy (mm), C_m is the maximum water storage of the canopy (mm) and ϵ_r is the fraction of the grid cell occupied by convective precipitation. The maximum amount of canopy water storage is a function of the leaf area index (L):

$$C_m = A_m + B_m L \tag{2}$$

where A_m is the ponding of water on the soil surface and interception by leafless vegetation (mm) and B_m is the rate of change of water holding capacity with leaf area index. At each timestep (n) the canopy storage is updated thus:

$$C^{(n+1)} = C^{(n)} + (P - T_F) \Delta t \tag{3}$$

Based on the surface energy balance, the fraction of the proportion of water stored in the canopy compared with the maximum canopy capacity of that plant type is used to calculate the effective surface resistance to determine tile evapotranspiration.

Surface runoff is generated by two processes in JULES: infiltration excess, where the water flux at the surface is greater than the infiltration rate of the soil, and saturated excess overland flow where the water flux at the surface is converted to runoff when the soil is completely saturated. To calculate the saturation-excess overland flow, the PDM⁶⁹ is used to determine the fraction of the model grid cell that will be saturated (f_{sat}) which is used as a multiplier to convert any excess water reaching the surface to runoff:

$$f_{\text{sat}} = 1 - \left[\frac{\max(0, S - S_0)}{S_{\text{max}} - S_0} \right]^b \tag{4}$$

where S is the fraction of the grid cell soil water storage, S_0 is the minimum storage at and below which there is no surface saturation (mm), S_{max} is the maximum grid cell storage (mm) and b is the Clapp and Hornberger⁷¹ soil exponent. We use the

topography-derived parameterisation for the b and S_0/S_{\max} parameters to reduce individual calibration with the following relationship⁵⁵:

$$\begin{cases} b = 2.0 \\ S_0/S_{\max} = \max(1 - \frac{s}{s_{\max}}, 0.0) \end{cases} \quad (5)$$

where s is the grid cell slope ($^\circ$) and s_{\max} is the maximum grid cell storage (mm). Once interception and surface runoff have been calculated, the remaining water enters the soil. This water is allocated to the different soil layers within the soil column by using the Darcy-Richards equation:

$$W = k \left(\frac{d\phi}{dz} + 1 \right) \quad (6)$$

where W is the vertical flux of water through the soil ($\text{kg m}^{-2} \text{s}^{-1}$), k is soil conductivity ($\text{kg m}^{-2} \text{s}^{-1}$), ϕ is suction (m) and z is the vertical flux of water through the soil (m). To calculate suction and soil conductivity, we use the van Genuchten⁷² scheme:

$$\left(\frac{\theta}{\theta_s} \right) = \frac{1}{[1 + (\alpha\phi)^{1-m}]^m} \quad (7)$$

where θ is the average volumetric soil moisture ($\text{m}^3 \text{m}^{-3}$), θ_s is the soil moisture at saturation ($\text{m}^3 \text{m}^{-3}$), α and m are van Genuchten parameters dependent on soil type. The hydraulic conductivity is calculated thus:

$$K_h = K_{hs} \varepsilon^e \left[1 - \left(1 - S^m \right)^{m-2} \right] \quad (8)$$

where K_h is the hydraulic conductivity (m s^{-1}) and K_{hs} is the hydraulic conductivity for saturated soil (m s^{-1}). ε is an empirical value set at 0.5 in JULES and S is found by:

$$S = \frac{(\theta - \theta_r)}{(\theta_s - \theta_r)} \quad (9)$$

where θ_r is the residual soil moisture ($\text{m}^3 \text{m}^{-3}$). Vegetation can access water from each level in the soil column as a function of the root density where the fraction of roots (r) in each soil layer (l) from depth z_{l-1} to z_l is:

$$r_l = \frac{e^{-\frac{2z_{l-1}}{d_r}} - e^{-\frac{2z_l}{d_r}}}{1 - e^{-\frac{2z_l}{d_r}}} \quad (10)$$

where z_l is the depth of the l th soil layer, d_r is the root depth (m) and z_l is the total depth of the soil column (m). The water flux extracted from a soil layer is $e_l E$ where E is transpiration ($\text{kg m}^{-2} \text{s}^{-1}$) and e_l can be found by:

$$e_l = \frac{r_l \beta_l}{\sum_l r_l \beta_l} \quad (11)$$

and β_l is defined by:

$$\beta_l = \begin{cases} 1 & \theta_l \geq \theta_c \\ (\theta_l - \theta_w) / (\theta_c - \theta_w) & \theta_w < \theta_l < \theta_c \\ 0 & \theta_l \leq \theta_w \end{cases} \quad (12)$$

where θ_c and θ_w are the volumetric soil moisture critical and wilting points respectively ($\text{m}^3 \text{m}^{-3}$) and θ_l is the unfrozen soil moisture at that soil layer ($\text{m}^3 \text{m}^{-3}$). In this configuration of JULES, when a soil layer becomes saturated, the excess water is routed to lower layers. When the bottom layer becomes fully saturated any excess water is added to the subsurface runoff. Both the surface and subsurface runoff are then passed to the River Flow Model^{65,73} which routes the flows according to a flow direction grid⁷⁴.

This study uses a combination of calibrated model parameters from the previous work of Robinson et al.⁵⁹ and Martinez-de la Torre et al.⁵⁵ (Rose suites u-bi090 and u-au394, respectively, which can be found using the Rose/Cyrc suite control system: <https://metomi.github.io/rose/doc/html/index.html>). We compare observed streamflow from the NRFA database⁷⁵ with model output for the years 2000–2010 using the base land and CHESS-met datasets. The model is spun-up for the years 1990–2000 to ensure soil moisture content has been equilibrated. To quantify the accuracy of the model, we use a range of standard error metrics. These include the Nash–Sutcliffe efficiency⁷⁶ measure:

$$\text{NSE} = 1 - \frac{\sum_{i=1}^n (Q_{\text{sim}} - Q_{\text{obs}})^2}{\sum_{i=1}^n (Q_{\text{obs}} - \bar{Q}_{\text{obs}})^2} \quad (13)$$

Kling–Gupta efficiency⁷⁷:

$$\text{KGE} = 1 - \sqrt{(r-1)^2 + \left(\frac{\sigma_{\text{sim}}}{\sigma_{\text{obs}}} - 1 \right)^2 + \left(\frac{\mu_{\text{sim}}}{\mu_{\text{obs}}} - 1 \right)^2} \quad (14)$$

Root-mean-squared error:

$$\text{RMSE} = \sqrt{\sum_{i=1}^n (Q_{\text{sim}} - Q_{\text{obs}})^2} \quad (15)$$

Mean absolute error:

$$\text{MAE} = \frac{\sum_{i=1}^n |Q_{\text{sim}} - Q_{\text{obs}}|}{n} \quad (16)$$

where Q_{sim} is the simulated discharge, Q_{obs} is the observed discharge, r is the linear correlation between observation and simulations, $\sigma_{\text{sim}/\text{obs}}$ is the standard deviation of discharge, $\mu_{\text{sim}/\text{obs}}$ is the mean of discharge and n is the number of observations. We also use NSE(log(Q)) and KGE(1/Q) to understand how well the model can reproduce low flows. Using these measures, we find that JULES performs satisfactorily apart from the Avon Catchment which may be due to fast subsurface flows generated by its geology⁵⁵ (Supplementary Table S7). With process-based models, it is difficult to both accurately reproduce physical processes and make the output faithful to reality due to epistemic uncertainties⁷⁸. Even though model performance is not the same as achieved with calibrated conceptual or empirical models, it allows us to determine the effects of vegetation changes on the hydrological cycle.

JULES' ability to faithfully represent hydrological land-surface processes in Great Britain has been evaluated in several studies^{58,79,80} and the plant functional type parameters it uses at global scales^{81,82}. To validate the ability of our configuration of JULES to represent soil moisture and potential evapotranspiration rates, we compare the model output with observations from twelve COSMOS-UK sites within our catchments covering grasslands, croplands, coniferous and broadleaf woodland⁸³ (Supplementary Fig. S8). We evaluate model performance from the start of the COSMOS-UK station records until January 1, 2018 so that we use the same forcing data as our experiments. Station start dates vary from October 2013 to August 2017. We compare COSMOS-UK observed soil moisture to the first 0.1 m of the soil column in JULES and evaporation to the sum of the soil evaporation and plant transpiration. We find a median KGE score of 0.44 for the topsoil moisture and 0.53 for potential evaporation (Supplementary Tables S9 and S10). Low error metrics observed for topsoil moisture are due to systematic undercalculation by JULES⁸⁰. At our broadleaf sites, Alice Holt and Wytham Woods, we find both systematic over and underprediction of the topsoil moisture respectively. In line with other studies, we find that there is a slight overestimation of evaporation in JULES^{58,84}. As illustrated by the median coefficients of determination between the COSMOS-UK and JULES data of 0.62 and 0.60 for the topsoil moisture and evaporation respectively, JULES broadly represents changes in these variables over time.

Land-cover scenarios. Modelling the influence of afforestation on catchment hydrology has been attempted before but usually only at the scale of a single catchment for a limited range of scenarios. In this study, we focus on the theoretical effect of widespread planting of broadleaf trees to examine whether planting location is a stronger control on hydrological response than afforestation extent by using a large ensemble of up to 288 land-cover change scenarios. We choose to focus just on broadleaf woodland for several reasons. First, we are trying to replicate a landscape that could be considered a natural climatic climax community that might occur if it had not been for human intervention during the Holocene. Second, broadleaf woodland has the potential to absorb and store carbon in soils for longer time periods. Finally, to reduce computational cost and the issue of potentially expanding the errors induced by potentially spurious parameters of needleleaf woodland in this version of JULES⁸⁵. Although potential woodland planting locations have been suggested by the Environment Agency and authorities in Scotland and Wales^{86–88}, the differences in planting criteria means it is not possible to systematically compare hydrological changes across our chosen catchments. Here we attempt to create afforestation scenarios related to both catchment river network structure and land use that are directly comparable across a range of catchments. Afforestation was in grassland areas to reduce the complexity of the decisions made and enable an understanding behind catchment sensitivity to land-cover changes related to soil and catchment structure.

Three metrics were selected to discretise the catchment into distinct areas for afforestation: the Topographic Wetness Index (TWI)²⁸, Strahler²⁷ and Shreve orders²⁶. These metrics capture different parts of the catchment such as propensity for saturation, drainage network location and relative contributing areas. TWI is calculated by:

$$\text{TWI} = \ln \frac{a}{\tan \gamma} \quad (17)$$

where a is the upslope area draining through a point, per unit contour length, and γ is the local surface topographic slope in radians. All three metrics were calculated using the 50 m IHDTM⁶⁰, thresholding stream formation at an accumulation of ten pixels using the D8 flow direction algorithm within ArcGIS 10.6.1⁸⁹. Strahler order ranges from one (headwaters) to seven (lowlands). Due to the continuous nature of TWI (0.05–31.49) and the large ordinal range of Shreve order (1–9523) calculated for the entire British Isles, we group TWI orders into five quantiles and seven quantiles for Shreve. Increasing TWI order in this case indicates increasing propensity for saturation, or potential maximum saturation level, and increasing Shreve order indicates increasing contributing area. Catchments were broken down to watersheds from the downstream point of the Shreve and Strahler orders. Due to the nature of the data, this led to some first order Strahler catchments being incorrectly generated for some catchments (Supplementary Table S7). Using these generated catchment areas, we plant both inside and outside of these watersheds to understand the hydrological difference between opposing planting locations. In each of the catchment areas, two different levels of afforestation were tested of ~25 and 50% of the possible planting area. Planted area was assigned at random in the

catchment and was produced by calculating the area available for afforestation and randomly producing points that covered the area required using the Create Random Points tool in ArcGIS 10.6.1.

Discussions exist about where to plant woodland in relation to existing land cover, to provide ecosystem services, including around watercourses^{29,30}, urban areas^{31,32} and woodland^{4,33}. Therefore, in this study we try to understand how these potential planting scenarios will affect hydrology in general. Using the CEH 2000 land-cover map⁵⁶ buffers of broadleaf land cover were created at 25 and 50 m around these three land uses (Supplementary Fig. S7). These were then discretised according to the catchment areas. As an example, one scenario would be afforesting up to 50 m around existing broadleaf woodland inside the Shreve order one catchment area, whilst another would be randomly afforesting within 25% of the available area outside of TWI order five areas.

Afforestation according to different catchment areas and land-cover uses between 234 and 288 scenarios for each catchment and between 0 and c. 40 percentage point increase in broadleaf woodland (Supplementary Fig. S2 and Table S8). Due to the structure and size of the different catchments, and thus differences in Strahler and Shreve orders, not all catchments had a comparable number of higher orders. Produced scenarios were converted to the 1-km² grid scale by altering the fraction of land-cover types within each grid cell. It should be noted that this work only considers the impact of mature broadleaf woodland and neglects the influence of the initial planting and growing of the woodland that would likely have its own impact on catchment hydrology as frequently reported^{13,49}. Furthermore, it does not include the period when there would be the highest amount of carbon sequestration. This study seeks to understand the theoretical impact of woodland on catchment hydrology when fully developed to understand the long-term implications of management decisions.

Hydrological signatures and analysis. Several hydrologic indices can be used to characterise the influence of afforestation on streamflow regime^{34,35}. To analyse average streamflow and extremes, we look at the top 1% (very high flow), 5% (high flow), 50% (median flow), 90% (low flow) and 95% (very low flow) quantiles of daily streamflow. To quantify flow variability, we use the slope of the flow duration curve^{38,40} calculated thus:

$$FDC = \frac{\ln(Q_{33\%}) - \ln(Q_{66\%})}{(0.66 - 0.33)} \quad (18)$$

where $Q_{33\%}$ is the 33rd flow exceedance quantile and $Q_{66\%}$ is the 66th flow exceedance quantile. To ascertain catchment responsiveness to climatic forcing, we use median streamflow elasticity^{40,41}:

$$MSE = \text{median} \left(\frac{dQ}{dP} \frac{P}{Q} \right) \quad (19)$$

where dQ and dP are the annual changes in yearly discharge and precipitation, respectively. Finally, we use the runoff ratio to quantify water balance changes related to streamflow and evapotranspiration⁴²:

$$RR = \frac{\mu_Q}{\mu_P} \quad (20)$$

where μ_Q and μ_P are the average yearly discharge and precipitation using daily values, respectively. We also qualitatively assess the largest peak flow daily event in the 10-year record used in this study to determine the impact of afforestation on the highest possible flows in each catchment.

To determine how afforestation influences streamflow metrics, percentage changes in flow metrics are plotted as a function of percentage point increases in afforestation (calculated using the difference between original and afforested scenario). Quantile regression is applied to determine the median regression slope of the trend for the entire period⁴³. The benefit of using quantile regression is that it identifies the median response of the input variable (in this case the level of afforestation in both percentage and absolute terms) without being influenced by extreme outliers. In this way, we can estimate the proportional streamflow response to afforestation over the period. We use the regression slope coefficient as a proxy of catchment sensitivity to afforestation for each streamflow metric. The slope coefficient is then correlated to catchment attributes, as stated in the CAMELS-GB dataset⁴⁴, using Spearman's rank correlation. This allows us to determine the direction and significance of the catchment property influences on the sensitivity of catchments to afforestation for the different hydrologic signatures. To determine the impact of different planting locations according to catchment and land-cover location a one-way analysis of variance (ANOVA) test is undertaken using R⁹⁰.

Data availability

Base model configuration used to run JULES can be found as Rose suite u-ce663 using the Rose/Cylc suite control system: <https://metomi.github.io/rose/doc/html/index.html>. Land-cover scenarios used to generate hydrologic implications of afforestation can be found on the Environmental Information Data Centre at <https://doi.org/10.5285/f484ff54-9139-462e-b37a-347a69f78500>. Generated data used for the creation of graphs can be found at <https://doi.org/10.5281/zenodo.5720264>.

Code availability

The code used to process the data and to produce the figures can be requested from the first author.

Received: 26 July 2021; Accepted: 16 December 2021;

Published online: 10 January 2022

References

- Lane, S. N. Natural flood management. *WIREs Water* **4**, e1211 (2017).
- Blöschl, G. et al. At what scales do climate variability and land cover change impact on flooding and low flows? *Hydrol. Process. An Int. J.* **21**, 1241–1247 (2007).
- Seddon, N. et al. Understanding the value and limits of nature-based solutions to climate change and other global challenges. *Philos. Trans. R. Soc. B Biol. Sci.* **375**, 20190120 (2020).
- Burton, V., Moseley, D., Brown, C., Metzger, M. J. & Bellamy, P. Reviewing the evidence base for the effects of woodland expansion on biodiversity and ecosystem services in the United Kingdom. *For. Ecol. Manage.* **430**, 366–379 (2018).
- Committee on Climate Change. Reducing UK emissions - 2019 Progress Report to Parliament. In *Progress Report to UK Parliament*. 93 (2020). <https://www.theccc.org.uk/publication/reducing-uk-emissions-2019-progress-report-to-parliament/%0Awww.theccc.org.uk/publications>.
- Committee on Climate Change. Net Zero: the UK's contribution to stopping global warming. In *Committee on Climate Change*. 275 (2019). <https://www.theccc.org.uk/publication/net-zero-the-uks-contribution-to-stopping-global-warming/>.
- Dadson, S. J. et al. A restatement of the natural science evidence concerning catchment-based 'natural' flood management in the UK. *Proc. R. Soc. A Math. Phys. Eng. Sci.* **473**, 20160706 (2017).
- Slater, L. et al. Global changes in 20-year, 50-year, and 100-year river floods. *Geophys. Res. Lett.* **48**, e2020GL091824 (2021).
- Griffin, A., Vesuviano, G. & Stewart, E. Have trends changed over time? A study of UK peak flow data and sensitivity to observation period. *Nat. Hazards Earth Syst. Sci.* **19**, 2157–2167 (2019).
- Gudmundsson, L., Leonard, M., Do, H. X., Westra, S. & Seneyratne, S. I. Observed trends in global indicators of mean and extreme streamflow. *Geophys. Res. Lett.* **46**, 756–766 (2019).
- Hannaford, J., Mastrantonas, N., Vesuviano, G. & Turner, S. An updated national-scale assessment of trends in UK peak river flow data: how robust are observed increases in flooding? *Hydrol. Res.* **52**, 699–718 (2021).
- Rogger, M. et al. Land use change impacts on floods at the catchment scale: challenges and opportunities for future research. *Water Resour. Res.* **53**, 5209–5219 (2017).
- Marc, V. & Robinson, M. The long-term water balance (1972–2004) of upland forestry and grassland at Plynlimon, mid-Wales. *Hydrol. Earth Syst. Sci.* **11**, 44–60 (2007).
- Bathurst, J. et al. Runoff, flood peaks and proportional response in a combined nested and paired forest plantation/peat grassland catchment. *J. Hydrol.* **564**, 916–927 (2018).
- Murphy, T. R., Hanley, M. E., Ellis, J. S. & Lunt, P. H. Native woodland establishment improves soil hydrological functioning in UK upland pastoral catchments. *L. Degrad. Dev.* <https://doi.org/10.1002/ldr.3762> (2020).
- Stratford, C. et al. Do trees in the UK-relevant river catchments influence fluvial flood peaks? <http://nora.nerc.ac.uk/517804/7/N517804CR.pdf> (2017).
- Carrick, J. et al. Is planting trees the solution to reducing flood risks? *J. Flood Risk Manag.* **12**, 1–10 (2019).
- Vertessy, R. A., Zhang, L. & Dawes, W. R. Plantations, river flows and river salinity. *Aust. For.* **66**, 55–61 (2003).
- Bathurst, J. C., Fahey, B., Iroumé, A. & Jones, J. Forests and floods: using field evidence to reconcile analysis methods. *Hydrol. Process.* **34**, 3295–3310 (2020).
- Slater, L. J. et al. Nonstationary weather and water extremes: a review of methods for their detection, attribution, and management. *Hydrol. Earth Syst. Sci.* **25**, 3897–3935 (2021).
- Zhang, M. et al. A global review on hydrological responses to forest change across multiple spatial scales: Importance of scale, climate, forest type and hydrological regime. *J. Hydrol.* **546**, 44–59 (2017).
- Zhou, G. et al. Global pattern for the effect of climate and land cover on water yield. *Nat. Commun.* **6**, 1–9 (2015).
- Best, M. J. et al. The Joint UK Land Environment Simulator (JULES), model description—Part 1: energy and water fluxes. *Geosci. Model Dev.* **4**, 677–699 (2011).
- Clark, D. B. et al. The Joint UK Land Environment Simulator (JULES), model description—Part 2: carbon fluxes and vegetation dynamics. *Geosci. Model Dev.* **4**, 701–722 (2011).

25. Thomson, A. et al. Quantifying the impact of future land use scenarios to 2050 and beyond. *Final Report for the Committee on Climate Change*. 78 (Centre for Ecology & Hydrology, 2018). <https://www.theccc.org.uk/wp-content/uploads/2018/11/Quantifying-the-impact-of-future-land-use-scenarios-to-2050-and-beyond-Full-Report.pdf>.
26. Shreve, R. L. Statistical law of stream numbers. *J. Geol.* **74**, 17–37 (1966).
27. Strahler, A. N. Quantitative analysis of watershed geomorphology. *Eos, Trans. Am. Geophys. Union* **38**, 913–920 (1957).
28. Beven, K. J. & Kirkby, M. J. A physically based, variable contributing area model of basin hydrology. *Hydrol. Sci. Bull.* **24**, 43–69 (1979).
29. Thomas, H. & Nisbet, T. R. An assessment of the impact of floodplain woodland on flood flows. *Water Environ. J.* **21**, 114–126 (2007).
30. de Sosa, L. L. et al. Delineating and mapping riparian areas for ecosystem service assessment. *Ecohydrology* **11**, 1–16 (2018).
31. Gunnell, K., Mulligan, M., Francis, R. A. & Hole, D. G. Evaluating natural infrastructure for flood management within the watersheds of selected global cities. *Sci. Total Environ.* **670**, 411–424 (2019).
32. Fuller, L., Marzano, M., Peace, A., Quine, C. P. & Dandy, N. Public acceptance of tree health management: results of a national survey in the UK. *Environ. Sci. Policy* **59**, 18–25 (2016).
33. Woodland Expansion Advisory Group. Report of the Woodland Expansion Advisory Group to the cabinet secretary for rural affairs and environment, Richard Lochhead MSP. 92 (2012). <http://scotland.foresstry.gov.uk/supporting/management/annual-review/woodland-expansion>.
34. Olden, J. D. & Poff, N. L. Redundancy and the choice of hydrologic indices for characterizing streamflow regimes. *River Res. Appl.* **19**, 101–121 (2003).
35. Addor, N., Newman, A. J., Mizukami, N. & Clark, M. P. The CAMELS data set: catchment attributes and meteorology for large-sample studies. *Hydrol. Earth Syst. Sci.* **21**, 5293–5313 (2017).
36. Wilby, R. L. & Quinn, N. W. Reconstructing multi-decadal variations in fluvial flood risk using atmospheric circulation patterns. *J. Hydrol.* **487**, 109–121 (2013).
37. Blöschl, G., Kiss, A., Viglione, A., Barriandos, M. & Böhm, O. Current European flood-rich period exceptional compared with past 500 years. *Nature* **583**, 560–566 (2020).
38. Yadav, M., Wagener, T. & Gupta, H. Regionalization of constraints on expected watershed response behavior for improved predictions in ungauged basins. *Adv. Water Resour.* **30**, 1756–1774 (2007).
39. Brown, A. E., Western, A. W., McMahon, T. A. & Zhang, L. Impact of forest cover changes on annual streamflow and flow duration curves. *J. Hydrol.* **483**, 39–50 (2013).
40. Sawicz, K., Wagener, T., Sivapalan, M., Troch, P. A. & Carrillo, G. Catchment classification: empirical analysis of hydrologic similarity based on catchment function in the eastern USA. *Hydrol. Earth Syst. Sci.* **15**, 2895–2911 (2011).
41. Sankarasubramanian, A., Vogel, R. M. & Limbrunner, J. F. Climate elasticity of streamflow in the United States. *Water Resour. Res.* **37**, 1771–1781 (2001).
42. Milly, P. C. D. Climate, soil water storage, and the average annual water balance. *Water Resour. Res.* **30**, 2143–2156 (1994).
43. Koehler, R. & Bassett, G. Regression quantiles. *Econometrica* **46**, 33 (1978).
44. Coxon, G. et al. CAMELS-GB: hydrometeorological time series and landscape attributes for 671 catchments in Great Britain. *Earth Syst. Sci. Data* **12**, 2459–2483 (2020).
45. Rinaldo, A., Marani, A. & Rigon, R. Geomorphological dispersion. *Water Resour. Res.* **27**, 513–525 (1991).
46. Rinaldo, A. & Rodriguez-Iturbe, I. Geomorphological theory of the hydrological response. *Hydrol. Process.* **10**, 803–829 (1996).
47. Afzal, M. & Ragab, R. Drought risk under climate and land use changes: implication to water resource availability at catchment scale. *Water* **11**, 1790 (2019).
48. Bentley, L. & Coomes, D. A. Partial river flow recovery with forest age is rare in the decades following establishment. *Glob. Chang. Biol.* **26**, 1458–1473 (2020).
49. Birkinshaw, S. J., Bathurst, J. C. & Robinson, M. 45 years of non-stationary hydrology over a forest plantation growth cycle, Coalburn catchment, Northern England. *J. Hydrol.* **519**, 559–573 (2014).
50. Jacob, O., Brown, I. & Rowan, J. Natural flood management, land use and climate change trade-offs: the case of Tarland catchment, Scotland. *Hydrol. Sci. J.* **62**, 1931–1948 (2017).
51. Wasko, C. et al. Incorporating climate change in flood estimation guidance. *Philos. Trans. A. Math. Phys. Eng. Sci.* **379**, 20190548 (2021).
52. Short, C., Clarke, L., Carnelli, F., Uttley, C. & Smith, B. Capturing the multiple benefits associated with nature-based solutions: lessons from a natural flood management project in the Cotswolds. *UK. L. Degrad. Dev.* **30**, 241–252 (2019).
53. Robinson, M. & Dupeyrat, A. Effects of commercial timber harvesting on streamflow regimes in the Plynlion catchments, mid-Wales. *Hydrol. Process.* **19**, 1213–1226 (2005).
54. Crooks, S. M., Kay, A. L., Davies, H. N. & Bell, V. A. From catchment to national scale rainfall-runoff modelling: Demonstration of a hydrological modelling framework. *Hydrology* **1**, 63–88 (2014).
55. Martínez-De La Torre, A., Blyth, E. M. & Weedon, G. P. Using observed river flow data to improve the hydrological functioning of the JULES land surface model (vn4.3) used for regional coupled modelling in Great Britain (UKC2). *Geosci. Model Dev.* **12**, 765–784 (2019).
56. Fuller, R. et al. Land cover map 2000—final report. <https://doi.org/10.5285/f802edfc-86b7-4ab9-b8fa-87e9135237c9> (2002).
57. Martínez-de la Torre, A., Blyth, E. M. & Robinson, E. L. Water, carbon and energy fluxes simulation for Great Britain using the JULES Land Surface Model and the Climate Hydrology and Ecology research Support System meteorology dataset (1961–2015) [CHESS-land]. (NERC Environmental Information Data Centre, 2018). <https://doi.org/10.5285/c76096d6-45d4-4a69-a310-4c67f8dcf096>.
58. Blyth, E. M., Martínez-de la Torre, A. & Robinson, E. L. Trends in evapotranspiration and its drivers in Great Britain: 1961 to 2015. *Prog. Phys. Geogr.* **43**, 666–693 (2019).
59. Robinson, E. L. et al. Climate hydrology and ecology research support system meteorology dataset for Great Britain (1961–2015) [CHESS-met] v1.2. NERC Environmental Information Data Centre. (Dataset). <https://doi.org/10.5285/b745e7b1-626c-4ccc-ac27-56582e77b900> (2017).
60. Morris, D. G. & Flavin, R. W. A digital terrain model for hydrology. *Proc 4th Int. Symp. Spat. Data Handl. Zürich* **1**, 250–262 (1990).
61. Wieder, W. R., Boehmert, J., Bonan, G. B. & Langseth, M. ReGRIDDED Harmonized World Soil Database v1.2. ORNL DAAC. <https://doi.org/10.3334/ORNLDAAAC/1247> (2014).
62. Robinson, E. L., Blyth, E. M., Clark, D. B., Finch, J. & Rudd, A. C. Trends in atmospheric evaporative demand in Great Britain using high-resolution meteorological data. *Hydrol. Earth Syst. Sci.* **21**, 1189–1224 (2017).
63. Paltan, H. et al. Global floods and water availability driven by atmospheric rivers. *Geophys. Res. Lett.* **44**, 10,387–10,395 (2017).
64. Gedney, N. et al. Detection of solar dimming and brightening effects on Northern Hemisphere river flow. *Nat. Geosci.* **7**, 796–800 (2014).
65. Dadson, S. J., Bell, V. A. & Jones, R. G. Evaluation of a grid-based river flow model configured for use in a regional climate model. *J. Hydrol.* **411**, 238–250 (2011).
66. Lewis, H. et al. The UKC3 regional coupled environmental prediction system. *Geosci. Model Dev.* **12**, 2357–2400 (2019).
67. Meier, R. et al. Empirical estimate of forestation-induced precipitation changes in Europe. *Nat. Geosci.* **14**, 473–478 (2021).
68. Fan, Y. et al. Hillslope hydrology in global change research and earth system modelling. *Water Resour. Res.* 1737–1772. <https://doi.org/10.1029/2018WR023903> (2019).
69. Clark, D. B. & Gedney, N. Representing the effects of subgrid variability of soil moisture on runoff generation in a land surface model. *J. Geophys. Res. Atmos.* **113**, 1–13 (2008).
70. Moore, R. J. The PDM rainfall-runoff model. *Hydrol. Earth Syst. Sci.* **11**, 483–499 (2007).
71. Clapp, R. B. & Hornberger, G. M. Empirical equations for some soil hydraulic properties. *Water Resour. Res.* **14**, 601–604 (1978).
72. van Genuchten, M. T. A closed-form equation for predicting the hydraulic conductivity of unsaturated soils. *Soil Sci. Soc. Am. J.* **44**, 892–898 (1980).
73. Bell, V. A., Kay, A. L., Jones, R. G. & Moore, R. J. Development of a high resolution grid-based river flow model for use with regional climate model output. *Hydrol. Earth Syst. Sci.* **11**, 532–549 (2007).
74. Davies, H. N. & Bell, V. A. Assessment of methods for extracting low-resolution river networks from high-resolution digital data. *Hydrol. Sci. J.* **54**, 17–28 (2009).
75. Vitolo, C., Fry, M. & Buytaert, W. Rnrf: An R package to retrieve, filter and visualize data from the UK national river flow archive. *R J.* **8**, 102–116 (2016).
76. Nash, J. E. & Sutcliffe, J. V. River flow forecasting through conceptual models part I—a discussion of principles. *J. Hydrol.* **10**, 282–290 (1970).
77. Gupta, H. V., Kling, H., Yilmaz, K. K. & Martinez, G. F. Decomposition of the mean squared error and NSE performance criteria: implications for improving hydrological modelling. *J. Hydrol.* **377**, 80–91 (2009).
78. Beven, K., Smith, P. J. & Wood, A. On the colour and spin of epistemic error (and what we might do about it). *Hydrol. Earth Syst. Sci.* **15**, 3123–3133 (2011).
79. Pinnington, E. et al. Improving soil moisture prediction of a high-resolution land surface model by parameterising pedotransfer functions through assimilation of SMAP satellite data. *Hydrol. Earth Syst. Sci.* **25**, 1617–1641 (2021).
80. Cooper, E. et al. Using data assimilation to optimize pedotransfer functions using field-scale in situ soil moisture observations. *Hydrol. Earth Syst. Sci.* **25**, 2445–2458 (2021).
81. Slevin, D., Tett, S. F. B. & Williams, M. Multi-site evaluation of the JULES land surface model using global and local data. *Geosci. Model Dev.* **8**, 295–316 (2015).
82. Harper, A. B. et al. Improved representation of plant functional types and physiology in the Joint UK Land Environment Simulator (JULES v4.2) using plant trait information. *Geosci. Model Dev.* **9**, 2415–2440 (2016).

83. Cooper, H. M. et al. COSMOS-UK: national soil moisture and hydrometeorology data for environmental science research. *Earth Syst. Sci. Data* **13**, 1737–1757 (2021).
84. Van den Hoof, C., Vidale, P. L., Verhoef, A. & Vincke, C. Improved evaporative flux partitioning and carbon flux in the land surface model JULES: impact on the simulation of land surface processes in temperate Europe. *Agric. For. Meteorol.* **181**, 108–124 (2013).
85. Broadmeadow, S., Thomas, H., Nisbet, T. & Valatin, G. Valuing flood regulation services of existing forest cover to inform natural capital accounts. *The Research Agency of the Forestry Commission*. 28 (2018). https://www.forestresearch.gov.uk/documents/5499/Final_report_valuing_flood_regulation_services_051218.pdf.
86. Broadmeadow, S., Thomas, H. & Nisbet, T. Opportunity mapping for woodland creation to reduce diffuse pollution and flood risk for England and Wales. *The Research Agency of the Forestry Commission*. https://www.forestresearch.gov.uk/documents/1768/FR_Broadmeadow_NOM_EW_2014.pdf, 41 (2014).
87. Sing, L., Metzger, M. J., Paterson, J. S. & Ray, D. A review of the effects of forest management intensity on ecosystem services for northern European temperate forests with a focus on the UK. *Forestry* **91**, 151–164 (2018).
88. Manzoor, S. A., Griffiths, G., Latham, J. & Lukac, M. Scenario-led modelling of broadleaf forest expansion in Wales. *R. Soc. Open Sci.* **6**, 190026 (2019).
89. O'Callaghan, J. F. & Mark, D. M. The extraction of drainage networks from digital elevation data. *Comput. Vision, Graph. Image Process.* **28**, 323–344 (1984).
90. RStudio Team. *RStudio: Integrated Development Environment for R* (RStudio, Inc., Boston, MA, 2021). <http://www.rstudio.com/>.

Acknowledgements

We thank Toby Marthews and Emma Robinson for assistance with the original configuration of the JULES model. The JASMIN CEDA service for access to facilities and resources. S.D. acknowledges funding from the UK Natural Environment Research Council (NE/S017380/1).

Author contributions

M.B., S.D. and L.S. co-designed the study. M.B. ran the simulations and analysed the results. All authors contributed to writing the manuscript.

Competing interests

The authors declare no competing interests.

Additional information

Supplementary information The online version contains supplementary material available at <https://doi.org/10.1038/s43247-021-00334-0>.

Correspondence and requests for materials should be addressed to Marcus Buechel.

Peer review information *Communications Earth & Environment* thanks Adriaan J. Teuling, David Scott and the other, anonymous, reviewer(s) for their contribution to the peer review of this work. Primary Handling Editors: Rahim Barzegar, Heike Langenberg. Peer reviewer reports are available.

Reprints and permission information is available at <http://www.nature.com/reprints>

Publisher's note Springer Nature remains neutral with regard to jurisdictional claims in published maps and institutional affiliations.



Open Access This article is licensed under a Creative Commons Attribution 4.0 International License, which permits use, sharing, adaptation, distribution and reproduction in any medium or format, as long as you give appropriate credit to the original author(s) and the source, provide a link to the Creative Commons license, and indicate if changes were made. The images or other third party material in this article are included in the article's Creative Commons license, unless indicated otherwise in a credit line to the material. If material is not included in the article's Creative Commons license and your intended use is not permitted by statutory regulation or exceeds the permitted use, you will need to obtain permission directly from the copyright holder. To view a copy of this license, visit <http://creativecommons.org/licenses/by/4.0/>.

© The Author(s) 2022